Received: 21 June 2022 | Revised: 7 August 2022 | Accepted: 9 August 2022

DOI: 10.1002/jcc.26995

RESEARCH ARTICLE

Journal of COMPUTATIONAL CHEMISTRY WILEY

Ligand-stabilized heteronuclear diatomics of group 13 and 15

Aishvaryadeep Kaur | David J. D. Wilson

Department of Biochemistry and Chemistry, La Trobe Institute of Molecular Science, La Trobe University, Melbourne, Victoria, Australia

Correspondence
David J. D. Wilson, Department of Biochemistry and Chemistry, La Trobe Institute of Molecular Science, La Trobe University, Melbourne, VIC 3086, Australia.
Email: david.wilson@latrobe.edu.au

Abstract

A theoretical investigation of ligand-stabilized MX diatomics (M = group 13, X = group 15 element) with *N*-heterocyclic carbene (NHC) ligands has been carried out to assess bonding and electronic structure. Binding of two ligands in the form L-MX-L is generally preferred over binding of a single ligand as L-MX or MX-L. Binding of carbene donor ligands is predicted to be thermodynamically favorable for all the systems, and is very favorable for the lighter group 15 systems (nitrogen and phosphorus). Detailed analysis of the bonding in these complexes has been carried out with energy decomposition analysis (EDA). In all cases, the carbene to boron and carbene to nitrogen bonding is described as an electron-sharing double bond with both σ and π bonding interactions. For the heavier elements, bonding to C (except for P—C interactions) is best described as a donor-acceptor σ single bond.

KEYWORDS
bonding, carbene ligands, electronic structure, group 13–15, ligand-stabilization

1 | INTRODUCTION

The combination of group 13 and 15 elements such as boron nitride (BN), boron arsenide (BAs), gallium nitride (GaN), and indium phosphide (InP) gives rise to valuable semiconductor and optoelectronics materials. Their utility for a range of applications may be related to their large electronic band gaps and chemical inertness properties. Moreover, these materials also have potential applications in hydrogen storage.[1–3] However, while their material forms are relatively common, their molecular forms remain elusive; those that have been isolated are only stable in a gaseous state at very high temperatures above 900°C, or in a condensed phase at temperatures below 40 K.[4–10]

Access to smaller molecular fragments of semiconductor and optoelectronic materials could aid in the tailored doping and construction of bulk materials.[11] Moreover, group 13–15 diatomic molecules are of inherent interest due to their elusive nature and close-lying ground state triplet and excited singlet electronic states.

Group 13–15 diatomics are challenging systems for both theory and experiment. Investigation of molecular forms of group 13–15 diatomics remains a challenge for both theory and experiment. Theoretical studies, often with multireference methods, have been carried out for a number of systems, including BN,[3,12–16] BP,[3,17,18] BAs,[19] AlN,[3,20] AlP,[3,21,22] AlAs,[23] GaN,[24,25] GaAs,[26] InN,[27] and InAs.[28]

Lewis bases such as *N*-heterocyclic carbenes (NHCs) offer great potential in this field due to their ability to activate and stabilize transient species, which could allow exploration of group 13–15 molecules (stabilized in a molecular form) while also offering a strategy to produce tailored fragments of bulk materials. Coordination with Lewis bases has propelled interest in main group chemistry,[29–31] with the fascinating reactivity and unusual bonding afforded by Lewis bases stimulating both experimentalists and theoreticians. Lewis bases have been demonstrated to provide access not only to transient molecular systems, but to rare low oxidation state systems, ions, and radicals.

Recent outstanding examples of Lewis-base stabilization include C_2,[32–37] Si_2,[38] Ge_2,[39] Sn_2,[40] B_2 (with the first B≡B bond),[41,42] Si_2O_4,[43] Be(0),[44] and Be(I)[45,46] complexes. A number of group 13 and 15 fragments have been stabilized in this manner, including N_2,[47–49] P_2,[50] As_2,[51] and phosphorus clusters P_1-P_4 and P_{12}.[50,52] To date, PN and

PN^+ remain the only heteronuclear group 15 systems to be isolated,[53] with a very recent report of a PN system stabilized by Fe.[54] Importantly, theoretical studies have often led synthetic efforts,[29,35,55–57] while theory has also proven critical for an understanding of the novel bonding in these systems.[57]

We have previously investigated group 14 and 15 L-E_2-L (L = ligand, E = C, Si, Ge, Si, Pb, N, P, As, Sb, Bi) complexes with NHC and phosphine ligands,[56] with group 15 systems exhibiting a gauche structure with E—E single bonds. Frenking and co-workers have previously investigated L-E_2-L (E = B, Al, Ga, In) with phosphine and NHC ligands,[57,58] predicting that all systems are energetically stable relative to 2 L + E_2. Recently, Rivard and Brown investigated L-$(BN)_n$ (n = 1–3) systems with NHC, *N*-heterocyclic olefin and Wittig ligand donors at the M05-2X/cc-pVTZ level of theory.[11]

Herein we report a theoretical study of heteronuclear diatomic MX species (M = Group 13 elements B, Al, Ga, In, Tl and X = Group 15 elements N, P, As, Sb, Bi) stabilized by NHC Lewis bases of the form L-MX-L, L-MX, and L-XM. Here we have investigated the electronic and thermodynamic stability of L-MX-L complexes, with a detailed analysis of the bonding. With the aid of energy decomposition analysis together with natural orbitals for chemical valence (EDA-NOCV), we have explored the strength and nature of the NHC to M and X bonds in both a donor–acceptor and electron-sharing paradigm.

2 | METHODS

Geometries were optimized with the M06-2X density functional[59] and def2-TZVP basis set[60] without any symmetry constraints using the Gaussian 16 package.[61] Functional dependence was assessed with B3LYP-D3(BJ)/def2-TZVP geometries for a set of the L-MX-L systems; B3LYP-D3(BJ) yielded equivalent geometries with bond distances deviating by less than 0.02 Å from M06-2X results. Harmonic vibration frequency calculations were performed analytically at the same level of theory as the geometry optimization to characterize each stationary point as a minima and obtain thermochemical data (standard state of T = 298.15 K and P = 1 atm). Dissociation energy calculations for L-MX-L complexes to MX + 2 L or L-MX + L or L + MX-L (L = NHC) employed L-MX-L (singlet), L-MX (singlet/triplet), MX-L (singlet), MX (triplet) and NHC (singlet) optimized geometries. Molecular orbital analysis including highest occupied molecular orbital-lowest unoccupied molecular orbital (HOMO-LUMO; H-L) gaps were calculated with B3LYP-D3(BJ)/def2-TZVP using the M06-2X/def2-TZVP optimized geometries. Analogous M06-2X/def2-TZVP MO results are given in Table S1. Singlet-triplet gaps were estimated from triplet state energies calculated at the singlet state optimized geometries at the M06-2X/def2-TZVP level.

EDA-NOCV was performed at the BP86/TZ2P level[62,63] using the ADF 2019 package.[64] Scalar relativistic effects were incorporated with the zeroth-order regular approximation. In EDA, the overall interaction energy between fragments (ΔE_{int}) may be decomposed into energy components:

$$\Delta E_{int} = \Delta E_{elstat} + \Delta E_{Pauli} + \Delta E_{orb} \quad (1)$$

where ΔE_{elstat} represents the electrostatic interaction energy between the unperturbed charge densities of the prepared fragments, which is generally a stabilizing force. The Pauli repulsion term (ΔE_{Pauli}) arises from antisymmetrization—the overlapping densities may have electrons that have the same spin, which then is corrected by introducing a destabilizing interaction. The orbital interaction energy (ΔE_{orb}) is an attractive term and represents the covalent interaction that originates from the mixing of orbitals, charge transfer, and polarization between the isolated fragments. Orbital mixing includes both inter-fragment and intra-fragment orbital mixing. Note that ΔE_{int} will differ from the dissociation energy since fragments are at the geometry of the complex are not relaxed to their ground states of the isolated fragments. With dispersion corrected functionals a dispersion contribution (ΔE_{disp}) is added to the interaction energy without impacting ΔE_{elstat}, ΔE_{Pauli}, or ΔE_{orb}. While BP86 does not include dispersion, test calculations with BP86-D3(BJ) for a subset of L-MX-L complexes indicates that dispersion adds 1%–6% to ΔE_{int}. Identification of the preferred bonding model is solely based on ΔE_{orb}, and hence is independent of whether dispersion is included. The ΔE_{orb} component may be further divided into contributions from each irreducible representation (σ, π, etc.). EDA-NOCV provides further insight by partitioning the total orbital interaction into pairwise orbital interactions. The deformation density $\Delta\rho(r)$, which is the difference between the charge densities of fragments before and after each orbital interaction, indicates charge flow due to orbital interactions.[65]

3 | RESULTS AND DISCUSSION

3.1 | Geometries

Several different arrangements of ligands (L) and diatomic MX can be envisaged. In a previous study of NHC stabilized BN fragments, Rivard and Brown considered L-BN structures with a single ligand.[11] We initially considered similar L-MX complexes of the form L-MX (ligand binding to group 13 element) or MX-L (ligand binding to group 15 element). However, complexes with two ligands of the form L_2-MX and L-MX-L are also possible. Calculations indicate that L-MX-L complexes are energetically preferred over an L_2-MX arrangement, while inclusion of two ligands in L-MX-L complexes is generally favored over a single ligand L-MX or MX-L structure (see below).

It is also possible to envisage MX complexes with three or even four ligands of the form L_2-MX-L_2. Three and four ligand complexes were investigated for the subset of BN, AlP, and GaAs diatomics at the M06-2X/def2-SVP level of theory. With four ligands no minimum energy structures were located but rather ligands dissociated, which is not unexpected due to significant steric crowding. Three-ligand L_2-MX-L structures were identified for both AlP and GaAs, which exhibit three-coordinate bonding around the group 13 element. In both cases the formation reaction of MX + 3 L → L_2-MX-L is energetically favored, although addition of a ligand to L-MX-L to form L_2-MX-L is mildly unfavorable. However, when the more synthetically

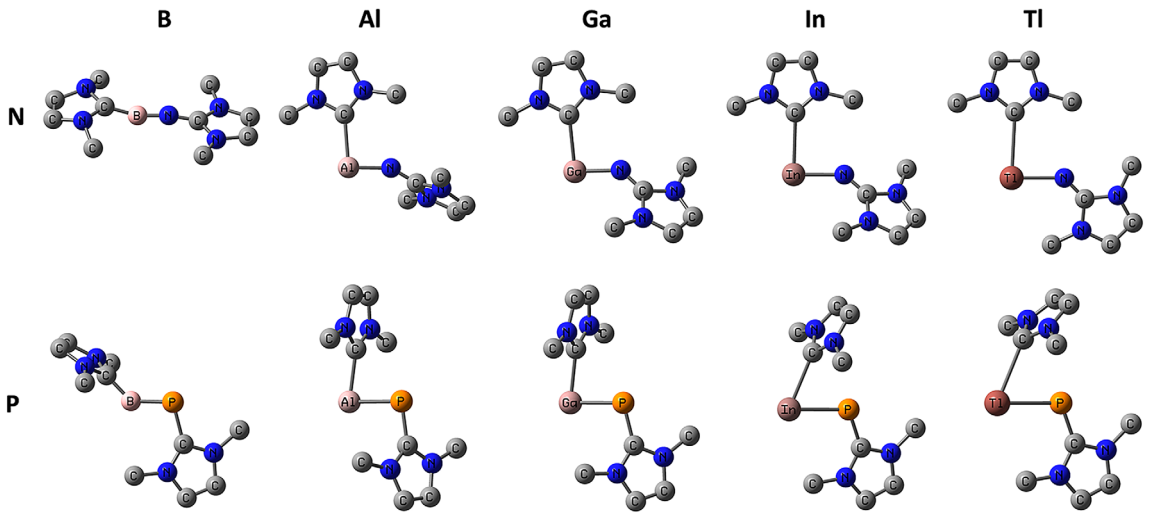

FIGURE 1 M06-2X/def2-TZVP optimized geometries of L-MX-L complexes (M = group 13 and X = N, P) in the gas phase (H atoms omitted for clarity). Geometries of the heavier group 15 complexes L-MX-L (X = As, Sb, Bi) are similar to the respective phosphorus complexes

relevant and bulkier *N*-dipp (dipp = diisopropylphenyl) NHC is used, neither three nor four ligand complexes could be formed due to the extreme steric crowding. The N-Me NHC ligands are a reasonable model for bulkier substituents, however synthetically relevant conclusions based on results with model N-Me NHCs requires the effect of bulky N-substituents to be considered. As such, the analysis presented here is principally focused on L-MX-L complexes.

The isoelectronic group 14 L-EE-L molecules (L = donor ligands; E = C, Si, Ge, Sn, Pb) are calculated to have a linear (E = C) or a *trans*-bent (E = Si-Pb) arrangement around the E—E core.[56] Similarly, homonuclear group 13 L-EE-L compounds (E = B-In) exhibit a linear (E = B) or *trans*-bent (E = Al-In) conformation,[57] while group 15 L-EE-L have a *trans*-bent (E = N-As) arrangement with bulky NHC ligands, or a gauche arrangement with less substituted (e.g., N-Me) NHC ligands.[56]

For the L-MX-L systems we considered linear, *trans*-bent, and gauche arrangements. The lowest energy optimized geometries of the singlet-state L-MX-L complexes (M = B, Al, Ga, In, Tl and X = N, P, As, Sb, Bi) are represented in Figure 1.

The heteronuclear MX complexes display a broader range of molecular structures than the homonuclear L-E_2-L complexes, often with a gauche arrangement around the M—X core with NHC rings that are not co-planar. This can be attributed to the asymmetric bonding nature of the MX linkages in these L-MX-L complexes in comparison to the homonuclear L-E_2-L systems. It is notable that the nitrogen containing L-MN-L complexes exhibit geometries that are different from their respective heavier complexes.

For complexes with at least one heavier element, multiple minima were located that correspond to a *cis* (same face) and *trans* (opposite face) arrangement of ligands around the MX core. The *cis* and *trans* minima typically lie within 15 kJ/mol of each other, with the *trans*-bent arrangement generally preferred. For GaN, InN, TlN, BBi, and TlP, a *cis* arrangement was found to be slightly lower in energy than a *trans*-bent geometry, although the difference in energy remained less than 10 kJ/mol.

Test calculations with *N*-dipp NHC ligands for GaN, InN, TlN, AlP, and GaAs demonstrate that only the *trans*-bent structure is feasible with synthetically relevant bulkier ligands due to significant steric repulsion in a *cis* arrangement. Moreover, for AlP and GaAs the bulkier *N*-dipp groups resulted in the NHC rings becoming co-planar. The key C—M, M—X, and X—C bond distances are largely unchanged whether N-Me or *N*-dipp groups are used, which confirms that the N-Me NHC ligands are a reasonable model. For consistency, the *trans*-bent conformation as illustrated in Figure 1 with N-Me NHC was utilized for all further analysis.

Selected geometry parameters of singlet-state L-MX-L complexes (M = B, Al, Ga, In, Tl and X = N, P, As, Sb, Bi) are collected in Table 1. The different structure of the L-BN-L complex is highlighted by the C—B—N (160.9°) and B—N—C (167.3°) angles, which are very different from that found in the heavier L-BX-L complexes (C—B—X = 130.4°–134.2° and B—X—C = 99.5°–102.9°). Comparison of the C—M—X and M—X—C angles of the heavier group 13-nitrogen complexes (M = Al-Tl) yields similar conclusions. The Ga, In, and Tl complexes with N appear to be reasonably similar in orientation; the C—M—X and M—X—C angles are in the range of 87.0°–91.8° and 134.7°–139.2°, respectively.

The bonding was analyzed separately for M—X bonds, carbene to group 13 metal (C—M) bonds, and carbene to group 15 non-metal (C—X) bonds in comparison with empirical covalent radii[66,67] and available experimental data.

3.2 | C—M bonds (M = B-Tl)

For the boron-containing L-BX-L complexes, the C—B bond increases monotonically from 1.440 to 1.484 Å with heavier group 15 elements (BN to BBi). The calculated C—B bond distances are comparable to 1.45 Å from Pyykko and Atsumi's covalent radii of C=B double bonds,[66] and also to recently isolated neutral boraalkene compounds

TABLE 1 M06-2X/def2-TZVP optimized geometries of NHC-MX-NHC systems (M = group 13, X = group 15) with selected geometrical parameters

	Bond distance (Å)			Angle (°)	
MX	C—M	M—X	X—C	C—M—X	M—X—C
BN	1.440	1.325	1.268	160.9	167.3
BP	1.475	1.786	1.830	134.2	102.9
BAs	1.481	1.896	1.986	130.4	100.7
BSb	1.483	2.065	2.270	132.0	101.2
BBi	1.484	2.121	2.428	131.8	99.5
AlN	2.261	1.801	1.264	94.3	150.3
AlP	2.123	2.346	1.789	82.4	97.4
AlAs	2.116	2.453	1.937	82.2	95.3
AlSb	2.105	2.645	2.193	81.3	96.7
AlBi	2.112	2.699	2.321	78.8	104.0
GaN	2.386	1.910	1.268	91.8	136.3
GaP	2.223	2.400	1.782	80.3	100.5
GaAs	2.211	2.503	1.931	80.0	98.5
GaSb	2.205	2.698	2.179	78.1	105.4
GaBi	2.204	2.741	2.314	77.7	103.6
InN	2.636	2.123	1.264	88.3	139.2
InP	2.540	2.642	1.766	71.7	113.9
InAs	2.535	2.733	1.913	71.6	111.2
InSb	2.521	2.910	2.167	71.9	107.4
InBi	2.530	2.944	2.302	71.0	105.9
TlN	2.801	2.252	1.262	87.0	134.7
TlP	2.722	2.725	1.760	69.6	113.4
TlAs	2.720	2.812	1.907	69.5	110.8
TlSb	2.710	2.985	2.161	69.9	107.1
TlBi	2.727	3.016	2.297	68.5	105.8

(1.444 Å, 1.456 Å).[68] For comparison, Rivard and Brown calculated a longer C—B bond distance of 1.517 Å in the single-ligand L-BN complex.[11] The C—B bond distances in L-BX-L are significantly shorter than reported C—B single bond distance of 1.592 Å, indicating the presence of double bond character in the C—B bond in the L-BX-L complexes.[69] The B—C bonds in L-BX-L are best described as B═C bonds.

In the non-boron L-MX-L complexes (M = Al-Tl), the calculated C—M bond distances (Table 1) consistently decrease with heavier group 15 elements (X = N—Bi), which is the reverse of the trend for C—B bond distances in L-BX-L complexes. All C—M bond distances are slightly longer than the C—M single bond covalent radii of Pyykko and Atsumi.[67] Moreover, the calculated bond distances are longer than experimentally reported C—M single bonds; C—Al bond distances (2.105–2.261 Å) are longer experimental C—Al values of 2.025–2.039 Å in L·AlH_2I complexes,[70] while optimized C—Ga bond distances (2.204–2.386 Å) are longer than 2.036 Å in L·GaH_2I.[70] Similarly, the optimized C—In (2.521–2.636 Å) and C—Tl (2.710–2.801 Å) bond distances are longer than C—M bond distances in aryl-NHC-group 13 trimethyl complexes of gallium and indium of 2.111–2.137 Å (C—In) and 2.301–2.342 Å (C—Tl), respectively.[71] A single-bond C—M (M = Al-Tl) description is consistent with the optimized bond distances.

3.3 | M—X bonds (M = B-Tl, X = N-Bi)

3.3.1 | B—X bond distances

The calculated B—N bond distance (1.325 Å) in L-BN-L lies between that of double bond as reported for $H_2N{=}BH_2$ (1.391 Å),[72] and a triple bond found in H—B≡N—H (1.238 Å).[73] Similarly, the calculated B—N bond distance lies between Pyykko's double bond covalent radii (1.38 Å) and triple bond covalent radii (1.27 Å). The B—N bond in L-BN-L may be characterized to possess significant triple bond character. For comparison, Rivard and Brown calculated a B—N bond distance of 1.259 Å in the single-ligand L-BN complex,[11] which is characterized as a distinct B≡N bond. The presence of the second ligand bound to N in L-BN-L serves to reduce the B—N bond strength, although it retains significant triple bond character in L-BN-L.

In contrast, the B—X bonds in the heavier group 15 homologues exhibit clear double bond character. The calculated B—P and B—As bond distances are comparable to B═P and B═As bonds in complexes reported by Power and co-workers[74] and Pyykko's double bond covalent radii of B═P (1.80 Å) and B═As (1.92 Å).[66] Similarly, the B—Sb and B—Bi distances are comparable to Pyykko's[67] double bond covalent radii (2.11, 2.19 Å respectively), while the B—Sb distance is shorter than experimentally known B—Sb single bonds[75,76] and the B-Bi distance is similar to experimental B═Bi distances (2.138 Å).[77] The B—X bonds of the heavier homologues are best described as B═X bonds.

3.3.2 | Al—X bond distances

The calculated Al—N bond distance (1.801 Å) in L-AlN-L is slightly shorter than reported Al—N single bond distances (>1.85 Å) but longer than 1.705 Å reported in monomeric iminoalane that contains multiple bond character.[78] It lies between the empirical double bond covalent radii of 1.73 Å and the single bond covalent radii of 1.97 Å,[66] which is indicative of minimal multiple bond character. For all other L-AlX-L molecules (X = P-Bi), the Al—X bond distances are consistent with known single bond distances: Al—P (L-AlP-L is 2.346 Å, cf. 2.37–2.39 Å),[67,79] Al—As (2.453 Å, cf. 2.42–2.50 Å),[67,80,81] Al—Sb (2.645 Å, cf. 2.66–2.68 Å),[67,82] and Al—Bi (2.699 Å, cf. 2.77 Å).[67] While Al—N may exhibit some double bond character, all heaver Al—X bonds are described as single bonds.

3.3.3 | Ga—X, In—X, and Tl—X bond distances

All Ga—X, In—X, and Tl—X bonds may be classified as single bonds. The Ga—N distance (1.910 Å) falls in the range of Ga—N single bonds

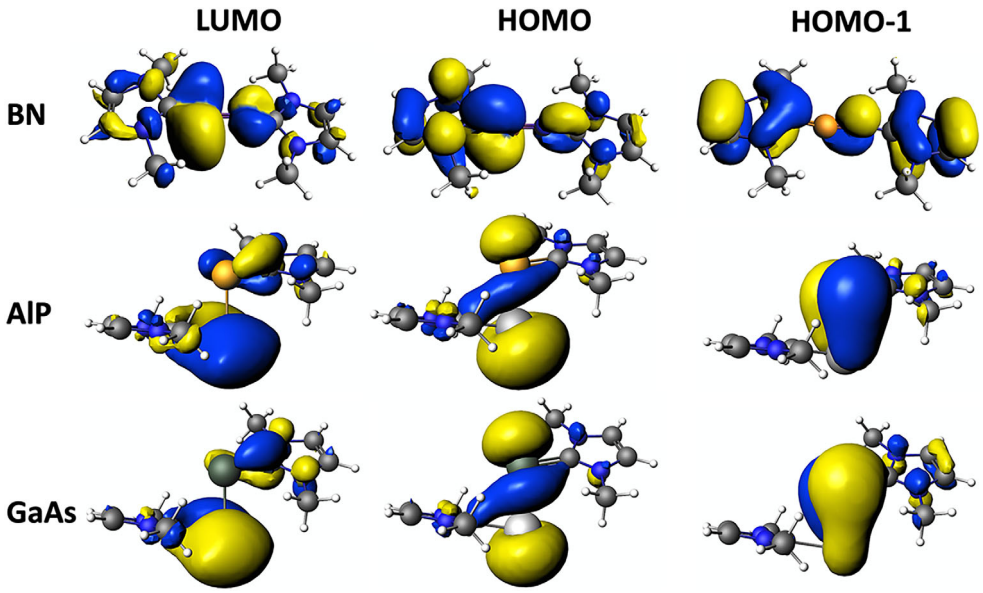

FIGURE 2 Plots of lowest unoccupied molecular orbital (LUMO), highest occupied molecular orbital (HOMO), and HOMO-1 of L-BN-L, L-AlP-L, and L-GaAs-L as representative of L-MX-L complexes. L = NHC, M = group 13, X = group 15 elements. B3LYP-D3(BJ)/def2-TZVP

(1.829–2.026 Å) found in gallium monoamides.[83] For the heavier homologues, calculated distances are similar to both empirical single-bond covalent radii and experimentally reported single bonds.[84] The In—N bond distance of 2.123 Å is similar to that in indium monoamides (2.054 Å, 2.104 Å),[83] while both In—N and In—Bi (2.944 Å) distances are also similar to single bond covalent radii (2.13 and 2.93 Å).[67] The In—P, In—As, and In—Sb distances are marginally longer than their respective single bond covalent radii: In—P 2.53 Å, In—As 2.63 Å, and In—Sb 2.82 Å.[67] The calculated Tl—X bond distances of are all slightly larger than their respective single bond covalent radii,[67] indicative of single-bond character.

3.4 | X—C bonds (X = N-Bi)

The calculated N—C bond distances are comparable to the N═C double bond covalent radii of 1.27 Å.[67] The calculated values are also slightly smaller than the known N—C bond distances in carbene stabilized PN (1.282 Å) and PN^+ (1.313 Å) complexes.[53] In all cases, the C—N bond distance is consistent with a C═N bond.

The P—C bond in L-BP-L (1.830 Å) is comparable to the P—C single bond covalent radii of 1.86 Å. However, in the heavier L-MP-L (M = Al-Tl) complexes, shorter P—C bond distances are predicted (1.789–1.760 Å) that lie between single bond (1.86 Å) and double bond (1.69 Å) covalent radii,[66,67] which is indicative of increased double-bond character. The calculated P—C bond distances are also comparable to distances in carbene-stabilized PN (1.719 Å) and PN^+ (1.788 Å) complexes.[53]

The As—C, Sb—C, and Bi—C are all consistent with a single bond description. The calculated As—C (1.907–1.986 Å) bond distances are comparable to those in NHC.$AsCl_3$ (2.018 Å) and NHC-AsAs-NHC (1.881 Å),[51] and the empirical single-bond covalent radii (1.96 Å) yet longer than double bond covalent radii (1.81 Å).[67] The Sb—C distances (2.161–2.270 Å) are comparable to known Sb—C single bonds (2.144–2.268 Å)[85] and empirical single bond covalent radii (2.00 Å).[67] Similarly, the calculated Bi—C bond distances (2.297–2.428 Å) are in agreement with known Bi—C bonds (2.339–2.489 Å).[85]

4 | ELECTRONIC STRUCTURE AND STABILITY

Plots of the frontier MOs of L-BN-L, L-AlP-L, and L-GaAs-L are presented in Figure 2, which are representative of the L-MX-L systems. For the non-nitrogen MX systems, the HOMO is an σ-symmetry bonding MO, while the HOMO-1 is a π-bonding MO centered on MX that is indicative of M═X bonding. The LUMO is a π-symmetry MO that is predominantly located on the group 15 X atom. For L-BN-L, the HOMO is associated with a B═C π-bond, while the π-symmetry HOMO-1 may be associated with B═N or a N lone pair.

The HOMO-LUMO (H-L) gap is commonly used as measure of the electronic stability of a system. However, it is important to note the strong density functional theory dependence of the calculated H-L gap, which increases with the proportion of Hartree–Fock exchange in the functional. The M06-2X functional includes a relatively high proportion of Hartree–Fock exchange (54%) that leads to large H-L gaps that generally overestimate experimental H-L gaps (photophysical, electrochemical). MO calculations were subsequently carried out at the B3LYP-D3(BJ)/def2-TZVP level of theory (20% Hartree–Fock exchange) that yields smaller H-L gaps. B3LYP-D3(BJ) calculated H-L gaps are provided in Table 2 (M06-2X results are provided in Table S5). The H-L gaps are in the range of 2.45–4.19 eV, indicating that these are potentially isolable based on calculations of known molecules.[56]

There are no clear trends in the H-L gaps for the L-MX-L complexes unless the nitrogen (MN) compounds are considered outliers. In this case the H-L gaps marginally increase in the boron complexes (from BP to BBi), while for the other series of group 13 element

TABLE 2 HOMO-LUMO gaps (H-L, eV, B3LYP-D3(BJ)/def2-TZVP//M06-2X/def2-TZVP) and singlet-triplet gaps (S-T, kJ/mol, M06-2X/def2-TZVP) of NHC-MX-NHC complexes; M = group 13, X = group 15 elements

BX	H-L	S-T	AlX	H-L	S-T	GaX	H-L	S-T	InX	H-L	S-T	TlX	H-L	S-T
BN	3.18	161.7	AlN	2.93	153.2	GaN	3.36	184.5	InN	3.27	195.9	TlN	3.26	257.2
BP	2.45	102.0	AlP	3.20	159.8	GaP	4.19	162.3	InP	2.99	157.2	TlP	3.01	183.4
BAs	2.57	107.6	AlAs	3.17	159.4	GaAs	3.21	160.5	InAs	2.94	211.7	TlAs	2.93	167.8
BSb	2.57	101.6	AlSb	3.01	150.5	GaSb	3.02	145.5	InSb	2.81	137.7	TlSb	2.79	143.6
BBi	2.72	110.1	AlBi	2.98	149.4	GaBi	3.03	141.5	InBi	2.79	150.3	TlBi	2.74	125.6

Abbreviations: HOMO, highest occupied molecular orbital; LUMO, lowest unoccupied molecular orbital.

TABLE 3 M06-2X/def2-TZVP calculated free energies (ΔG_{298K}, kJ/mol) of reaction for 2 NHC (singlet) + MX (triplet) → NHC-MX-NHC (singlet); M = group 13, X = group 15 elements

BX		AlX		GaX		InX		TlX	
BN	−490.3	AlN	−504.7	GaN	−476.6	InN	−465.6	TlN	−448.2
BP	−378.4	AlP	−304.2	GaP	−277.5	InP	−262.0	TlP	−251.2
BAs	−343.0	AlAs	−250.6	GaAs	−222.9	InAs	−181.4	TlAs	−166.9
BSb	−323.5	AlSb	−190.8	GaSb	−155.5	InSb	−137.7	TlSb	−126.7
BBi	−291.6	AlBi	−155.2	GaBi	−117.4	InBi	−65.7	TlBi	−87.1

complexes (AlX, GaX, InX, TlX) there is a general trend that the H-L gap decreases with heavier group 15 elements. For all series of group 15 complexes (MN, MP, MAs, MSb, MBi) there is no discernable trend as a function of group 13 partner with the exception that the H-L gap is always a maximum with Ga. Based on H-L gaps, the L-GaX-L (X = N-Bi) would appear to be the most electronically stable of the complexes considered.

To further test the electronic stability, approximate singlet-triplet energy gaps were calculated from triplet state energies calculated at the singlet state optimized geometries at the M06-2X/def2-TZVP level (Table 2). In all cases the singlet-triplet gap is greater than 100 kJ/mol, indicative that all complexes have a stable singlet ground state.

5 | THERMODYNAMIC STABILITY

The thermodynamic stability was then evaluated by calculating ΔG_{298K} for complexation from separate MX diatomics and two NHC ligands,

$$2\,\mathrm{NHC} + \mathrm{MX} \rightarrow \mathrm{NHC} - \mathrm{MX} - \mathrm{NHC} \quad (2)$$

Results are presented in Table 3. The bare MX diatomic systems are known to possess significant multireference character.[3,12–28] For all L-MX-L systems the multireference character was analyzed from the T1 diagnostic[86,87] calculated at the CCSD/def2-SVP level of theory using the M06-2X/def2-TZVP geometries. In all cases the T1 diagnostic is less than 0.02, indicative of the suitability of single reference methods as employed in this study (Table S4).

In all cases the reactions are calculated to be exergonic, indicating that binding of two donor ligands is thermodynamically favorable for all systems. The calculated ΔG for nitrogen complexes L-MN-L are the largest in magnitude (−448.3 to −504.7 kJ/mol), with L-AlN-L being the most thermodynamically stable system (−504.7 kJ/mol) relative to MX + 2 L. Indeed, the calculated ΔG values are larger than 100 kJ/mol for all complexes except for L-InBi-L (−65.7 kJ/mol) and L-TlBi-L (−87.1 kJ/mol). There is a consistent trend for each series of group 13 complexes (columns in Table 3), with the magnitude of ΔG decreasing on moving down group 15, with the ΔG for bismuth complexes being the smallest in magnitude in each column.

The relative stability of complexes with one or two ligands was also explored via

$$\mathrm{NHC} + \mathrm{MX} \rightarrow \mathrm{NHC} - \mathrm{MX} \quad (3)$$

$$\mathrm{NHC} + \mathrm{MX} \rightarrow \mathrm{MX} - \mathrm{NHC} \quad (4)$$

$$\mathrm{NHC} - \mathrm{MX} + \mathrm{NHC} \rightarrow \mathrm{NHC} - \mathrm{MX} - \mathrm{NHC} \quad (5)$$

$$\mathrm{NHC} + \mathrm{MX} - \mathrm{NHC} \rightarrow \mathrm{NHC} - \mathrm{MX} - \mathrm{NHC} \quad (6)$$

Results for complexation with a single ligand (Equations 3 and 4) are collected in Table 4, while results for further complexation of a second ligand (Equations 5 and 6) are presented in Table 5.

It is notable that while all NHC-MX-NHC and NHC-XM complexes possess a singlet ground state, the situation is quite different for the NHC-MX complexes. All NHC-BX complexes exhibit a singlet ground state, while the heavier group 13 NHC-MX complexes predominantly have triplet ground states; all In and Tl complexes are triplet ground states, while Al and Ga complexes with P and As are singlets but with N, Sb, and Bi are triplets.

Formation of single-ligand complexes (Equations 3 and 4, Table 4) is calculated to be energetically favorable in all cases. Somewhat surprisingly, for the single-ligand complexes NHC-MX and NHC-XM, binding of NHC to the group 15 element (X) is generally favored over

TABLE 4 M06-2X/def2-TZVP calculated free energies (ΔG_{298K}, kJ/mol) for reaction of NHC + MX, with M = group 13, X = group 15 elements

NHC (singlet) + MX (triplet) → NHC-MX (singlet/triplet)								
BX		**AlX**		**GaX**		**InX**		**TlX**	
BN	−431.7	AlN[a]	−94.2	GaN[a]	−69.5	InN[a]	−66.0	TlN[a]	−38.3
BP	−404.8	AlP	−120.4	GaP	−104.6	InP[a]	−56.6	TlP[a]	−35.1
BAs	−375.1	AlAs	−109.5	GaAs	−88.2	InAs[a]	−32.3	TlAs[a]	−30.3
BSb	−337.4	AlSb[a]	−92.5	GaSb[a]	−70.6	InSb[a]	−49.8	TlSb[a]	−40.4
BBi	−314.1	AlBi[a]	−89.3	GaBi[a]	−68.3	InBi[a]	−42.1	TlBi[a]	−40.8
NHC (singlet) + MX (triplet) → MX-NHC (singlet)								
BX		**AlX**		**GaX**		**InX**		**TlX**	
BN	−441.9	AlN	−504.0	GaN	−481.4	InN	−462.5	TlN	−443.1
BP	−184.6	AlP	−248.0	GaP	−247.0	InP	−234.9	TlP	−239.6
BAs	−141.7	AlAs	−189.5	GaAs	−185.9	InAs	−157.0	TlAs	−145.6
BSb	−93.2	AlSb	−117.4	GaSb	−112.4	InSb	−105.4	TlSb	−99.7
BBi	−58.5	AlBi	−80.1	GaBi	−73.8	InBi	−36.2	TlBi	−68.0

[a]NHC-MX complex has a triplet ground state.

TABLE 5 M06-2X/def2-TZVP calculated free energies (ΔG_{298K}, kJ/mol) for the listed reactions, with M = group 13, X = group 15 elements

NHC-MX (singlet/triplet) + NHC (singlet) → NHC-MX-NHC (singlet) (Equation 5)								
BX		**AlX**		**GaX**		**InX**		**TlX**	
BN	−58.6	AlN[a]	−410.4	GaN[a]	−407.1	InN[a]	−399.6	TlN[a]	−409.9
BP	26.5	AlP	−183.8	GaP	−172.9	InP[a]	−205.3	TlP[a]	−216.1
BAs	32.2	AlAs	−141.1	GaAs	−134.8	InAs[a]	−149.1	TlAs[a]	−136.5
BSb	13.8	AlSb[a]	−98.4	GaSb[a]	−84.8	InSb[a]	−87.9	TlSb[a]	−86.3
BBi	22.5	AlBi[a]	−65.9	GaBi[a]	−49.0	InBi[a]	−23.6	TlBi[a]	−46.3
MX-NHC (singlet) + NHC (singlet) → NHC-MX-NHC (singlet) (Equation 6)								
BX		**AlX**		**GaX**		**InX**		**TlX**	
BN	−48.4	AlN	−0.7	GaN	4.8	InN	−3.1	TlN	−5.1
BP	−193.7	AlP	−56.2	GaP	−30.5	InP	−27.1	TlP	−11.6
BAs	−201.3	AlAs	−61.1	GaAs	−37.1	InAs	−24.4	TlAs	−21.3
BSb	−230.3	AlSb	−73.4	GaSb	−43.1	InSb	−32.3	TlSb	−26.9
BBi	−233.1	AlBi	−75.1	GaBi	−43.6	InBi	−29.5	TlBi	−19.0

[a]NHC-MX complex has a triplet ground state.

binding to the more electropositive group 13 element (M). As a donor-acceptor complex, it would be expected that a Lewis base (NHC) would preferentially bind to the more electropositive group 13 element. For the important BN system, the M06-2X/def2-TZVP results indicate that NHC-NB is lower in energy than NHC-BN by 6.2 (ΔE_e) and 10.2 kJ/mol (ΔG). Rivard and Brown have previously carried out a detailed study of NHC-BN complexes,[11] however it is unclear whether they considered the NHC-NB conformation. The M06-2X/def2-TZVP calculated ΔG for NHC + BN → NHC-BN of −431.7 kJ/mol is significantly smaller in magnitude than the M05-2X/cc-pVTZ value of −548.5 kJ/mol reported by Rivard and Brown, with high-level calculations appearing to be necessary to provide quantitative results of the global minima and energy difference between NHC-BN and NHC-NB. Regardless, the present results indicate that the NHC-BN and NHC-NB conformations lie very close in energy, with the two-ligand NHC-BN-NHC complex being more energetically stable than both NHC-BN and NHC-NB (Equations 5 and 6).

For all other boron complexes the NHC-BX conformation is very strongly favored (>200 kJ/mol) over NHC-XB, which is the expected result for a donor-acceptor complex with electron-deficient boron. The only other complexes for which an NHC-MX conformation is more stable are AlBi and InBi. The exception for BN is indicative of the strong C—N bond formed in NHC-NB that is stronger than a simple donor-acceptor interaction (see below). This is further evidenced by the NHC-NX conformation being more stable than NHC-XN by 394–412 kJ/mol for X = Al-Tl.

Complexation of a second ligand (Equations 5 and 6) is thermodynamically favorable with few exceptions. For complexes with elements

from the third period or heavier (Al-Tl and P-Bi), both reactions (5) and (6) are exergonic, indicative of the preference for product formation with two ligands. With boron, all NHC + BX-NHC reactions (Equation 6) are calculated to be favorable, however for NHC-BX + NHC (Equation 5) only NHC-BN preferably binds two ligands; with X = P-Bi the binding of a second ligand is endergonic. This is consistent with the very strong preference of NHC-BX over an BX-NHC arrangement, and indicative of weaker C—X bonding in these systems in comparison with the C═N bonding in BN-NHC. Indeed, all MN complexes differ from the general trends for Equations (5) and (6). The calculated ΔG for NHC + MN-NHC (Equation 6) with M = Al-Tl are in the range of −5.1 to +4.8 kJ/mol, which is indicative of minimal or no stability gain with the addition of a second ligand.

6 | BONDING

The intriguing trends in bond distances and energetics of the L-MX-L complexes encouraged us to probe the nature of the element-ligand interaction using EDA-NOCV. The traditional approach would be to consider two fragments (two NHCs as one fragment and diatomic MX as a separate fragment) or three fragments (each NHC as a fragment and MX as a fragment). However, the lack of symmetry and more complex electronic environment led to SCF convergence issues and significant technical complexities in obtaining correct fragment electronic states with both fragmentation approaches. As a result, separate EDA calculations were carried out to analyze C—X and C—M bonding independently. To analyze C—X bonding, fragments of NHC-MX and NHC were utilized, while fragments of NHC and MX-NHC were utilized to probe C—M bonding. In each case both donor-acceptor (DA, closed-shell singlet state fragments) and electron-sharing (ES, open-shell fragments) bonding models were considered. EDA-NOCV analysis further enabled the orbital interaction (ΔE_{orb}) to be separated into σ and π contributions, although since the L-MX-L complexes are asymmetric the assignment of σ or π is based on the symmetry of the NHC orbital involved in the orbital interaction. Numerical EDA results are provided in Tables 6 and 7 for M = B, Al, Ga, while the C—In, C—Tl, C—Sb, C—Bi results are presented in Tables S2 and S3. In a small number of cases, EDA results for the DA bonding model could not be obtained as the required fragment orbital occupation led to extreme SCF convergence issues, however bonding trends indicate that in each of these cases the ES model is the preferred model.

6.1 | C—M bonding (NHC + MX-NHC)

6.1.1 | Boron complexes (M = B)

The numerical EDA results for C—B bonding (NHC to BX-NHC) indicate that an electron-sharing model is the preferred bonding description, as indicated by a smaller magnitude ΔE_{orb} term (Table 6). For example, in the L-BP-L system the ΔE_{orb} term for donor-acceptor and electron-sharing is −264.3 and −192.3 kcal/mol, respectively. The total interaction energy (ΔE_{int}) is substantial, ranging from −163.7 to −168.7 kcal/mol. Of the stabilizing components of the interaction (ΔE_{orb} and ΔE_{elstat}), in all cases the orbital term makes the largest contribution (53.9%–56.3%) compared to the electrostatic component (43.7%–46.1%), which is consistent with significant covalent character of the C—B bond. Moreover, the ΔE_{orb} contributions contain substantial σ (58.8%–66.9%) as well as π (26.0%–34.5%) components. The nature of the orbital interaction is highlighted with NOCV deformation density plots in Figure 3. Both numerical results and NOCV plots make it evident that there is significant C═B character, consistent with calculated bond distances.

6.1.2 | Non-boron complexes (M = Al-Tl)

In contrast to the boron complexes, in the non-boron complexes EDA analysis indicates that the C—M interaction is better described by a donor–acceptor bonding model (Tables 6 and S2). For example, EDA results analysis of the C—Al bond in the L-AlP-L system yields ΔE_{orb} values for the donor-acceptor and electron-sharing bonding model of −61.9 and −163.4 kcal/mol, respectively. The overall interaction of the NHC ligand with heavier MX-NHC (−10.4 to −31.7 kcal/mol) complexes is much weaker compared than in the BX-NHC fragment.

For each series of group 13 complexes, ΔE_{int} consistently increases in magnitude moving down group 15. For example, in the aluminum complexes, ΔE_{int} increases from −12.8 kcal/mol (AlN complex) to −31.7 kcal/mol (AlBi complex) with the carbene forms the strongest interaction with the AlBi-NHC fragment. Unlike in L-BX-L systems, the electrostatic interactions (60.5%–66.9%) make a significant contribution to the overall attraction in these systems, which is indicative of the ionic nature of these interactions.

No π back-donation was observed from EDA-NOCV analysis of pairwise orbital interactions, while σ-contribution to orbital interactions ranges from 59.7% to 76.7% in these systems, consistent with a C—M single bond.

6.2 | X—C bonding (NHC-MX + NHC)

Numerical results for EDA calculations are provided in Table 7 for X = N, P, and As, with the X = Sb, Bi results presented in Table S3.

6.2.1 | Nitrogen complexes (X = N)

The overall interaction energies of the N—C electron-sharing bond in L-MN-L complexes (Table 7) range from −196.4 to −201.6 kcal/mol, with the L-BN-L system having the largest interaction energy. As expected, the orbital component is the largest contributor (63.2%–64.8%) to the total attractive interaction energy, with a smaller electrostatic component (35.2%–36.8%). Thus, all N—C interactions have a predominant covalent character. There are both σ (56.9%–65.9%) and π (22.4%–31.5%) symmetry orbital contributions to ΔE_{orb}, which is consistent with the C═N double bond description based on analysis of bond distances.

TABLE 6 Computed EDA–NOCV components (in kcal/mol) for the C—B, C—Al, C—Ga bonds of the NHC-MX-NHC systems at the BP86/TZ2P level of theory

C—B	N		P		As		Sb		Bi	
	DA	**ES**	DA	**ES**	DA	**ES**	DA	**ES**	DA	**ES**
ΔE_{int}	-	−163.7	−160.9	−168.4	−155.4	−168.0	−140.4	−168.7	−131.8	−166.6
ΔE_{Pauli}		194.4	329.0	188.1	369.5	189.4	374.9	188.8	377.2	193.4
ΔE_{elstat}[a]		−163.6 (45.7%)	−225.6 (46.1%)	−164.2 (46.1%)	−239.7 (45.7%)	−162.6 (45.5%)	−235.8 (45.8%)	−158.3 (44.3%)	−231.9 (45.6%)	−157.3 (43.7%)
ΔE_{orb}[a]		−194.5 (54.3%)	−264.3 (53.9%)	−192.3 (53.9%)	−285.2 (54.3%)	−194.8 (54.5%)	−279.5 (54.2%)	−199.1 (55.7%)	−277.2 (54.4%)	−202.8 (56.3%)
$\Delta E_{orb,\rho_1}$[b]		−118.2 (60.8%)		−113.1 (58.8%)		−120.4 (61.8%)		−130.9 (65.8%)		−135.5 (66.9%)
$\Delta E_{orb,\rho_2}$[b]		−60.0 (30.8%)		−66.4 (34.5%)		−61.4 (31.5%)		−54.7 (27.5%)		−52.8 (26.0%)
C—Al	**N**		**P**		**As**		**Sb**		**Bi**	
	DA	ES	**DA**	ES	**DA**	ES	**DA**	ES	**DA**	ES
ΔE_{int}	−12.8	−204.7	−25.5	−202.9	−27.1	−203.2	−31.2	−203.3	−31.7	−202.7
ΔE_{Pauli}	116.9	146.2	133.8	141.3	135.5	144.8	139.7	148.5	143.1	155.1
ΔE_{elstat}[a]	−79.5 (61.3%)	−190.8 (54.4%)	−97.3 (61.1%)	−180.8 (52.5%)	−99.3 (61.1%)	−183.4 (52.7%)	−103.4 (60.5%)	−185.6 (52.7%)	−106.0 (60.6%)	−192.3 (53.8%)
ΔE_{orb}[a]	−50.2 (38.7%)	−160.1 (45.6%)	−61.9 (38.9%)	−163.4 (47.5%)	−63.3 (38.9%)	−164.6 (47.3%)	−67.5 (39.5%)	−166.3 (47.3%)	−68.8 (39.4%)	−165.5 (46.2%)
$\Delta E_{orb,\rho_1}$[b]	−37.3 (74.2%)		−42.7 (69.0%)		−42.0 (66.4%)		−41.7 (61.7%)		−41.1 (59.7%)	
$\Delta E_{orb,\rho_2}$[b]										
C—Ga	**N**		**P**		**As**		**Sb**		**Bi**	
	DA	ES	**DA**	ES	**DA**	ES	**DA**	ES	**DA**	ES
ΔE_{int}	−10.8	−202.7	−19.7	−199.1	−21.0	−199.1	−23.7	−198.9	−24.7	−197.8
ΔE_{Pauli}	93.6	111.1	116.5	119.5	119.4	123.2	124.5	130.6	125.5	133.4
ΔE_{elstat}[a]	−65.2 (62.5%)	−166.2 (53.0%)	−86.3 (63.4%)	−169.9 (53.3%)	−89.2 (63.5%)	−172.2 (53.4%)	−93.6 (63.1%)	−178.9 (54.3%)	−95.0 (63.3%)	−180.7 (54.6%)
ΔE_{orb}[a]	−39.2 (37.5%)	−147.6 (47.0%)	−49.9 (36.6%)	−148.7 (46.7%)	−51.2 (36.5%)	−150.0 (46.6%)	−54.6 (36.9%)	−150.5 (45.7%)	−55.2 (36.7%)	−150.4 (45.4%)
$\Delta E_{orb,\rho_1}$[b]	−30.0 (76.7%)		−37.7 (75.6%)		−37.7 (73.6%)		−38.8 (71.1%)		−37.6 (68.3%)	
$\Delta E_{orb,\rho_2}$[b]										

Note: Fragments of NHC and MX-NHC with donor-acceptor (DA) and electron-sharing (ES) bonding models. The preferred bonding model is indicated in bold.

[a]Values in parentheses are the percentage contribution to the attractive interaction, which is $\Delta E_{elstat} + \Delta E_{orb}$.

[b]The values in parentheses show the contribution to the total orbital interaction ΔE_{orb}.

TABLE 7 Computed EDA–NOCV components (in kcal/mol) for N—C_{NHC}, P—C_{NHC}, As—C_{NHC} bonds of the NHC-MX-NHC systems at the BP86/TZ2P level of theory

N—C	B		Al		Ga		In		Tl	
	DA	**ES**	DA	**ES**	DA	**ES**	DA	**ES**	DA	**ES**
ΔE_{int}	-	−201.6	-	−196.4	−124.5	−197.6	−165.9	−200.5	−145.0	−196.8
ΔE_{Pauli}		422.5		470.9	1097.2	445.8	1128.5	457.8	1079.1	568.7
ΔE_{elstat}[a]		−222.8 (35.7%)		−244.8 (36.7%)	−433.9 (35.5%)	−229.0 (35.6%)	−447.3 (34.6%)	−231.7 (35.2%)	−431.3 (35.2%)	−281.7 (36.8%)
ΔE_{orb}[a]		−401.4 (64.3%)		−422.6 (63.3%)	−787.8 (64.5%)	−414.4 (64.4%)	−847.2 (65.4%)	−426.6 (64.8%)	−792.8 (64.8%)	−483.8 (63.2%)
$\Delta E_{orb}, \rho_1$[b]		−255.1 (63.6%)		−241.3 (57.1%)		−239.7 (57.8%)		−242.7 (56.9%)		−318.6 (65.9%)
$\Delta E_{orb}, \rho_2$[b]		−90.0 (22.4%)		−124.8 (29.5%)		−124.6 (30.1%)		−134.4 (31.5%)		−111.4 (23.0%)
P—C	**B**		**Al**		**Ga**		**In**		**Tl**	
	DA	**ES**	**DA**	**ES**	**DA**	**ES**	DA	**ES**	**DA**	ES
ΔE_{int}	−22.2	−192.4	−62.3	−209.9	−70.1	−214.4	−79.0	−217.1	−83.7	−220.1
ΔE_{Pauli}	393.1	258.4	372.0	244.1	365.7	244.5	390.0	247.2	333.2	246.0
ΔE_{elstat}[a]	−209.5 (50.5%)	−242.1 (53.7%)	−215.6 (49.7%)	−236.2 (52.0%)	−215.4 (49.4%)	−237.7 (51.8%)	−226.2 (48.2%)	−235.3 (50.7%)	−206.0 (49.4%)	−236.3 (50.7%)
ΔE_{orb}[a]	−205.7 (49.5%)	−208.6 (46.3%)	−218.7 (50.3%)	−217.8 (48.0%)	−220.4 (50.6%)	−221.2 (48.2%)	−242.7 (51.8%)	−229.0 (49.3%)	−211.0 (50.6%)	−229.8 (49.3%)
$\Delta E_{orb}, \rho_1$[b]	−164.8 (80.1%)	−153.8 (73.7%)	−168.6 (77.1%)	−154.4 (70.9%)	−166.8 (75.7%)	−154.4 (69.8%)	−180.3 (74.3%)	−155.8 (66.2%)	−150.9 (71.5%)	−112.3 (47.5%)
$\Delta E_{orb}, \rho_2$[b]	−14.8 (7.2%)	−23.7 (11.4%)	−21.9 (10.0%)	−29.0 (13.3%)	−24.0 (10.9%)	−32.9 (14.9%)	−24.4 (10.1%)	−37.8 (16.1%)	−27.7 (13.1%)	−20.4 (8.6%)
As—C	**B**		**Al**		**Ga**		**In**		**Tl**	
	DA	ES	**DA**	ES	**DA**	ES	**DA**	ES	**DA**	ES
ΔE_{int}	−16.9	−186.4	−51.9	−198.9	−58.7	−203.0	−66.4	−205.1	−69.9	−207.7
ΔE_{Pauli}	312.1	201.2	300.0	193.4	292.0	191.9	308.5	196.9	266.0	196.1
ΔE_{elstat}[a]	−181.0 (55.0%)	−213.0 (55.0%)	−192.7 (54.8%)	−209.7 (53.5%)	−191.9 (54.7%)	−210.0 (53.2%)	−201.3 (53.7%)	−209.9 (52.2%)	−186.2 (55.4%)	−210.9 (52.2%)
ΔE_{orb}[a]	−147.9 (45.0%)	−174.6 (45.0%)	−159.2 (45.2%)	−182.6 (46.5%)	−158.9 (45.3%)	−184.8 (46.8%)	−173.6 (46.3%)	−192.0 (47.8%)	−149.8 (44.6%)	−192.9 (47.8%)
$\Delta E_{orb}, \rho_1$[b]	−119.1 (80.5%)		−123.9 (77.9%)		−121.2 (76.3%)		−129.2 (74.4%)		−106.9 (71.4%)	
$\Delta E_{orb}, \rho_2$[b]	−10.8 (7.3%)		−15.0 (9.4%)		−16.8 (10.6%)		−18.7 (10.8%)		−21.3 (14.2%)	

Note: Fragments of NHCMX and NHC with donor-acceptor (DA) and electron-sharing (ES) bonding models. The preferred bonding model is indicated in bold.

[a]Values in parentheses are the percentage contribution to the attractive interaction, which is $\Delta E_{elstat} + \Delta E_{orb}$.

[b]The values in parentheses show the contribution to the total orbital interaction ΔE_{orb}.

6.2.2 | Phosphorus complexes (X = P)

In boron, aluminum, and gallium complexes of phosphorus, the P—C interaction could be equally described with a donor-acceptor or an electron-sharing bonding description as the difference in the ΔE_{orb} term is less than 3 kcal/mol (Table 7). For the donor acceptor approach, the overall interaction energy increases in magnitude going down the group, from −22.2 kcal/mol (L-BP-L) to −70.1 kcal/mol (L-GaP-L). For the electron-sharing bonding model, the overall interaction between the charged fragments is much larger in comparison with the donor acceptor approach. However, there is a comparatively smaller increase in the overall interaction energy on moving down the group 13 (−192.4 kcal/mol for L-BP-L, −209.9 kcal/mol for L-AlP-L, and −214.4 kcal/mol for L-GaP-L). In both donor-acceptor and electron-sharing bonding models, the percentage electrostatic contribution slightly decreases, and percentage orbital interaction slightly increases down the group for both the bonding models (Table 7). However, the electrostatic (ionic) and orbital (covalent) interaction are calculated to both contribute nearly 50% to the overall attractive forces. In the donor-acceptor bonding model, the σ component forms the major orbital interaction (71.5%–80.1%), and decreases as we move down the group 13, and inversely the less significant π component (7.2%–13.1%) becomes more prominent for the heavier group 13 complexes. This is consistent with the analysis based on bond distances, that π character is more dominant in the heavier group 13 complexes.

The nature of P—C interactions in the indium and thallium complexes is different from other P—C interactions. The P—C interaction in the L-InP-L complex could be better described by an electron-sharing bonding model with the ΔE_{orb} term −229.0 kcal/mol (ΔE_{orb} term for donor-acceptor approach is −242.7 kcal/mol). The overall interaction energy of the fragments (−217.1 kcal/mol) is higher compared to the L-GaP-L complex. The σ component forms 66.2% of the total orbital interaction and there is a prominent π component as well. For the L-TlP-L complex, the P—C interaction could be better described as a donor-acceptor interaction ΔE_{orb} term for the donor-acceptor model is −211.0 kcal/mol and electron-sharing is −229.8 kcal/mol. The electrostatic and orbital interactions were each calculated to give nearly 50% contribution to the overall attractive forces. Considering the major orbital interactions, σ-donation is the major orbital interaction (71.5%) followed by π back donation (13.1%).

6.2.3 | Other complexes (X = As-Bi)

Comparing the ΔE_{orb} term in each case, the carbene carbon to XM-NHC interaction in arsenic, antimony, and bismuth complexes could be better described by the donor-acceptor bonding model (Tables 7 and S3). For example, in the L-BAs-L molecule, analyzing the As—C bond, the ΔE_{orb} contribution for the donor–acceptor model is −147.9 kcal/mol and for the electron-sharing model is −174.6 kcal/mol.

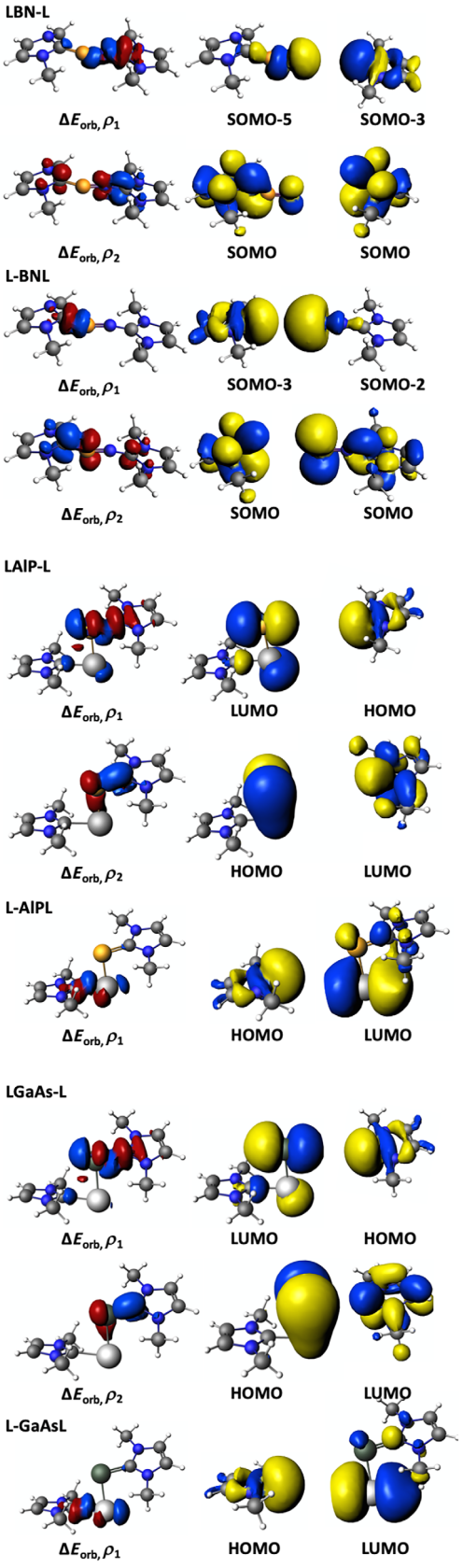

FIGURE 3 Natural orbitals for chemical valence (NOCV) deformation density plots of key orbital interactions in NHC + MX-NHC and NHC-MX + NHC. Charge flow is from red to blue

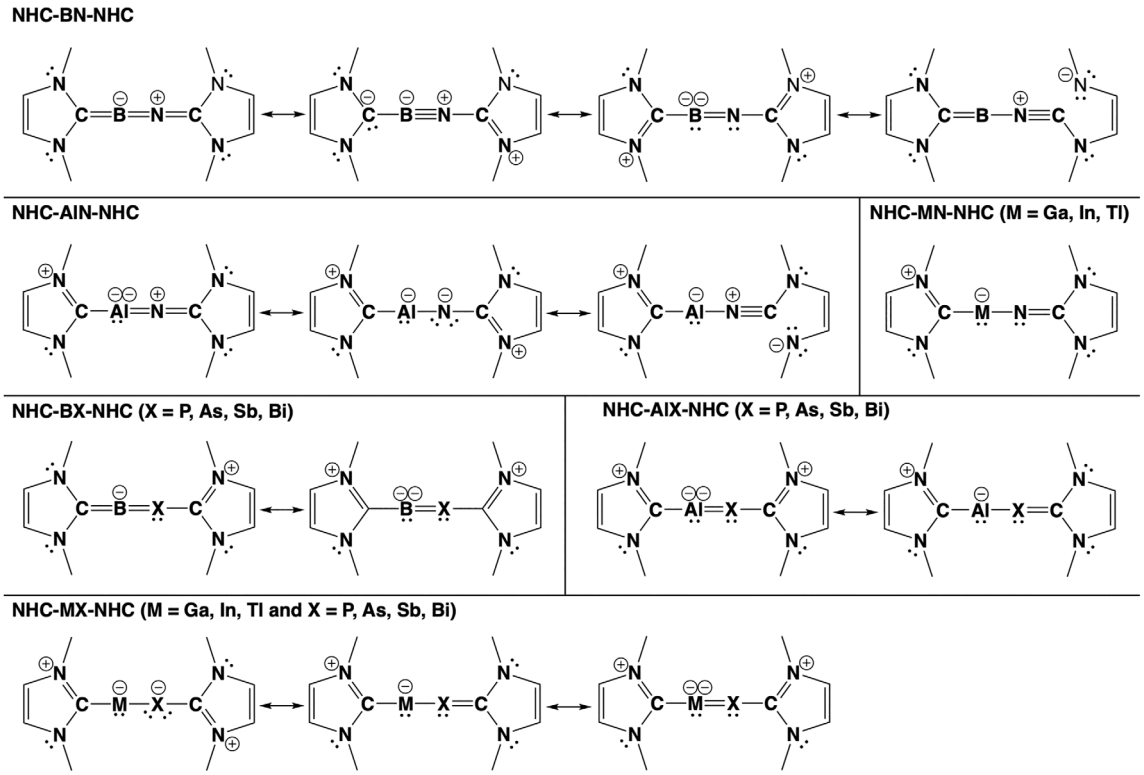

FIGURE 4 Best Lewis depictions of the bonding in L-MX-L (M = group 13, X = group 15 elements) based on results from geometry and bonding analysis

In each group 15 case, the overall interaction energy for the preferred bonding model increases down group 13. For example, in the L-MAs-L complexes, the interaction energy increases from −16.9 kcal/mol in the boron complex to −69.9 kcal/mol in the thallium complex of arsenic. In all these complexes, the C—As interaction is the strongest with $\Delta E_{int} = -69.9$ kcal/mol. It is reflected from the percentage values, the contribution from the electrostatic interactions is larger than the contribution from orbital interactions toward the total attractive forces in all cases. For example, in As—C interaction, electrostatic interactions contribute 53.7%–55.4%, whereas orbital interactions contribute 44.6%–46.3% toward the total attractive interaction. The percentage electrostatic contribution increases, and orbital contribution decreases on moving down the group 15. This indicates that Bi—C interaction has more ionic character than Sb—C interaction which in turn has more ionic character than As—C interaction. Consistent with a single bond description, σ-donation is the major orbital interaction. The percentage σ-donation decreases down the group 13. For example, L-BAs-L (80.5% σ-donation) and L-TlAs-L (71.4% σ-donation).

6.3 | Bonding summary

The best Lewis description of the electronic structures of L-MX-L based on bond distance and bonding analysis (EDA, NBO, MO) is shown in Figure 4. It is emphasized that the Lewis description is a simplification of the true electron distribution due to significant delocalization, however it is instructive to highlight the diversity of bonding in these systems.

7 | CONCLUSIONS

From a thorough theoretical investigation it is predicted that group 13–15 heteronuclear diatomics are stabilized by NHC donor ligands, with all L-MX-L complexes calculated to be thermodynamically and electronically stable compounds. It is predicted that the molecular form of these important materials could be synthetically isolable with appropriate ligands. The nitrogen and phosphorus complexes are comparatively more stable than the heavier group 15 complexes. Analysis of the nature of carbene to group 13 metal and carbene to group 15 bonding revealed that nitrogen and boron atoms form an electron-sharing double bond with carbene carbon, and in both these cases contribution from both σ and π symmetry fragment orbitals of NHC was observed. However, the interaction between the heavier group 13 and 15 atoms with NHC donor ligand (except the P—C interaction) could be described as a donor-acceptor single bond with σ-donation being the major orbital interaction.

ACKNOWLEDGMENTS

We thank the National Computational Infrastructure National Facility (NCI-NF), Intersect, and La Trobe University for high-performance

computing resources. Open access publishing facilitated by La Trobe University, as part of the Wiley - La Trobe University agreement via the Council of Australian University Librarians.

DATA AVAILABILITY STATEMENT

The data that support the findings of this study are available in the SI with any additional data available from the corresponding author upon request.

ORCID

David J. D. Wilson https://orcid.org/0000-0002-0007-4486

REFERENCES

[1] D. J. Grant, D. A. Dixon, *J. Phys. Chem. A* **2005**, *109*, 10138.
[2] D. A. Dixon, M. Gutowski, *J. Phys. Chem. A* **2005**, *109*, 5129.
[3] Z. Gan, D. J. Grant, R. J. Harrison, D. A. Dixon, *J. Chem. Phys.* **2006**, *125*, 124311.
[4] S. Li, R. J. Van Zee, W. Weltner, *J. Phys. Chem.* **1994**, *98*, 2275.
[5] M. Lorenz, J. Agreiter, A. M. Smith, V. E. Bondybey, *J. Chem. Phys.* **1996**, *104*, 3143.
[6] K. A. Gingerich, *J. Chem. Phys.* **1972**, *56*, 4239.
[7] J. A. Perri, S. La Placa, B. Post, *Acta Cryst.* **1958**, *11*, 310.
[8] M. Ebben, J. J. ter Meulen, *Chem. Phys. Lett.* **1991**, *177*, 229.
[9] G. Meloni, K. A. Gingerich, *J. Chem. Phys.* **2000**, *113*, 10978.
[10] J. D. Simmons, J. K. McDonald, *J. Mol. Spectrosc.* **1972**, *41*, 584.
[11] M. R. Momeni, L. Shulman, E. Rivard, A. Brown, *Phys. Chem. Chem. Phys.* **2015**, *17*, 16525.
[12] J. M. L. Martin, T. J. Lee, G. E. Scuseria, P. R. Taylor, *J. Chem. Phys.* **1992**, *97*, 6549.
[13] C. W. Bauschlicher, H. Partridge, *Chem. Phys. Lett.* **1996**, *257*, 601.
[14] A. Karton, J. M. L. Martin, *J. Chem. Phys.* **2006**, *125*, 144313.
[15] X. Li, J. R. Gour, J. Paldus, P. Piecuch, *Chem. Phys. Lett.* **2008**, *461*, 321.
[16] D. Shi, W. Xing, H. Liu, J. Sun, Z. Zhu, Y. Liu, *Spectrochim. Acta A* **2012**, *93*, 367.
[17] R. Linguerri, N. Komiha, R. Oswald, A. Mitrushchenkov, P. Rosmus, *Chem. Phys.* **2008**, *346*, 1.
[18] B. Miguel, S. Omar, P. Mori-Sánchez, J. M. G. de la Vega, *Chem. Phys. Lett.* **2003**, *381*, 720.
[19] I. Magoulas, A. Kalemos, *J. Chem. Phys.* **2013**, *139*, 154309.
[20] A. Kalemos, A. Mavridis, *J. Phys. Chem. A* **2007**, *111*, 11221.
[21] P. J. Bruna, F. Grein, *J. Phys. B: At. Mol. Opt. Phys.* **1989**, *22*, 1913.
[22] U. Meier, S. D. Peyerimhoff, P. J. Bruna, S. P. Karna, F. Grein, *Chem. Phys.* **1989**, *130*, 31.
[23] E. F. Archibong, A. St-Amant, *Chem. Phys. Lett.* **2002**, *355*, 249.
[24] D. Tzeli, A. A. Tsekouras, *J. Chem. Phys.* **2008**, *128*, 144103.
[25] P. A. Denis, K. Balasubramanian, *Chem. Phys. Lett.* **2006**, *423*, 247.
[26] U. Meier, S. D. Peyerimhoff, P. J. Bruna, F. Grein, *J. Mol. Spectrosc.* **1989**, *134*, 259.
[27] L. Demovič, I. Černušák, G. Theodorakopoulos, I. D. Petsalakis, M. Urban, *Chem. Phys. Lett.* **2007**, *447*, 215.
[28] A. Dutta, D. Giri, K. K. Das, *J. Phys. Chem. A* **2001**, *105*, 9049.
[29] D. J. D. Wilson, J. L. Dutton, *Chem. – Eur. J.* **2013**, *19*, 13626.
[30] N. M. Scott, S. P. Nolan, *Eur. J. Inorg. Chem.* **2005**, *2005*, 1815.
[31] W. A. Herrmann, *Angew. Chem., Int. Ed.* **2002**, *41*, 1290.
[32] S. M. N. V. T. Gorantla, S. Pan, K. C. Mondal, G. Frenking, *J. Phys. Chem. A* **2021**, *125*, 291.
[33] L. Jin, M. Melaimi, L. L. Liu, G. Bertrand, *Org. Chem. Front.* **2014**, *1*, 351.
[34] G. Frenking, S. Shaik, *The Chemical Bond: Fundamental Aspects of Chemical Bonding*, John Wiley & Sons, Inc., Weinheim, Germany **2014**.
[35] J. L. Dutton, D. J. D. Wilson, *Angew. Chem. Int. Ed.* **2012**, *51*, 1477.
[36] D. C. Georgiou, B. D. Stringer, C. F. Hogan, P. J. Barnard, D. J. D. Wilson, N. Holzmann, G. Frenking, J. L. Dutton, *Chem. – Eur. J.* **2015**, *21*, 3377.
[37] T.-F. Leung, D. Jiang, M.-C. Wu, D. Xiao, W.-M. Ching, G. P. A. Yap, T. Yang, L. Zhao, T.-G. Ong, G. Frenking, *Nat. Chem.* **2021**, *13*, 89.
[38] Y. Wang, Y. Xie, P. Wei, R. B. King, H. F. Schaefer, P. Von, R. Schleyer, G. H. Robinson, *Science* **2008**, *321*, 1069.
[39] A. Sidiropoulos, C. Jones, A. Stasch, S. Klein, G. Frenking, *Angew. Chem. Int. Ed.* **2009**, *48*, 9701.
[40] C. Jones, A. Sidiropoulos, N. Holzmann, G. Frenking, A. Stasch, *Chem. Commun.* **2012**, *48*, 9855.
[41] H. Braunschweig, D. Dewhurst Rian, K. Hammond, J. Mies, K. Radacki, A. Vargas, *Science* **2012**, *336*, 1420.
[42] G. Frenking, N. Holzmann, *Science* **2012**, *336*, 1394.
[43] Y. Wang, M. Chen, Y. Xie, P. Wei, H. F. Schaefer Iii, P. V. R. Schleyer, G. H. Robinson, *Nat. Chem.* **2015**, *7*, 509.
[44] M. Arrowsmith, H. Braunschweig, M. A. Celik, T. Dellermann, R. D. Dewhurst, W. C. Ewing, K. Hammond, T. Kramer, I. Krummenacher, J. Mies, K. Radacki, J. K. Schuster, *Nat. Chem.* **2016**, *8*, 890.
[45] G. Wang, J. E. Walley, D. A. Dickie, S. Pan, G. Frenking, R. J. Gilliard, *J. Am. Chem. Soc.* **2020**, *142*, 4560.
[46] S. A. Couchman, N. Holzmann, G. Frenking, D. J. D. Wilson, J. L. Dutton, *Dalton Trans.* **2013**, *42*, 11375.
[47] R. Appel, R. Schöllhorn, *Angew. Chem. Int. Ed.* **1964**, *3*, 805.
[48] M. Reinmuth, C. Neuhäuser, P. Walter, M. Enders, E. Kaifer, H.-J. Himmel, *Eur. J. Inorg. Chem.* **2011**, *2011*, 83.
[49] N. Holzmann, D. Dange, C. Jones, G. Frenking, *Angew. Chem. Int. Ed.* **2013**, *52*, 3004.
[50] Y. Wang, Y. Xie, P. Wei, R. B. King, H. F. Schaefer, P. V. R. Schleyer, G. H. Robinson, *J. Am. Chem. Soc.* **2008**, *130*, 14970.
[51] M. Y. Abraham, Y. Wang, Y. Xie, P. Wei, H. F. Schaefer III, P. V. R. Schleyer, G. H. Robinson, *Chem. – Eur. J.* **2010**, *16*, 432.
[52] O. Back, G. Kuchenbeiser, B. Donnadieu, G. Bertrand, *Angew. Chem. Int. Ed.* **2009**, *48*, 5530.
[53] R. Kinjo, B. Donnadieu, G. Bertrand, *Angew. Chem. Int. Ed.* **2010**, *49*, 5930.
[54] A. K. Eckhardt, M.-L. Y. Riu, M. Ye, P. Müller, G. Bistoni, C. C. Cummins, *Nat. Chem.* **2022**, *14*, 928.
[55] D. M. Andrada, G. Frenking, *Angew. Chem. Int. Ed.* **2015**, *54*, 12319.
[56] D. J. D. Wilson, S. A. Couchman, J. L. Dutton, *Inorg. Chem.* **2012**, *51*, 7657.
[57] N. Holzmann, A. Stasch, C. Jones, G. Frenking, *Chem. – Eur. J.* **2011**, *17*, 13517.
[58] N. Holzmann, A. Stasch, C. Jones, G. Frenking, *Chem. – Eur. J.* **2013**, *19*, 6467.
[59] Y. Zhao, D. G. Truhlar, *Theor. Chem. Acc.* **2008**, *120*, 215.
[60] F. Weigend, R. Ahlrichs, *Phys. Chem. Chem. Phys.* **2005**, *7*, 3297.
[61] M. J. Frisch, G. W. Trucks, H. B. Schlegel, G. E. Scuseria, M. A. Robb, J. R. Cheeseman, G. Scalmani, V. Barone, G. A. Petersson, H. Nakatsuji, X. Li, M. Caricato, A. V. Marenich, J. Bloino, B. G. Janesko, R. Gomperts, B. Mennucci, H. P. Hratchian, J. V. Ortiz, A. F. Izmaylov, J. L. Sonnenberg, D. Williams-Young, F. Ding, F. Lipparini, F. Egidi, J. Goings, B. Peng, A. Petrone, T. Henderson, D. Ranasinghe, V. G. Zakrzewski, J. Gao, N. Rega, G. Zheng, W. Liang, M. Hada, M. Ehara, K. Toyota, R. Fukuda, J. Hasegawa, M. Ishida, T. Nakajima, Y. Honda, O. Kitao, H. Nakai, T. Vreven, K. Throssell, J. A. Montgomery Jr., J. E. Peralta, F. Ogliaro, M. J. Bearpark, J. J. Heyd, E. N. Brothers, K. N. Kudin, V. N. Staroverov, T. A. Keith, R. Kobayashi, J. Normand, K. Raghavachari, A. P. Rendell, J. C. Burant, S. S. Iyengar, J. Tomasi, M. Cossi, J. M. Millam, M. Klene, C. Adamo, R. Cammi, J. W. Ochterski, R. L. Martin, K. Morokuma, O. Farkas, J. B. Foresman, D. J. Fox, *Gaussian 16, Revision E.01*, Gaussian, Inc., Wallingford, CT **2016**.
[62] A. D. Becke, *Phys. Rev. A* **1988**, *38*, 3098.
[63] J. P. Perdew, *Phys. Rev. B* **1986**, *33*, 8822.

[64] G. te Velde, F. M. Bickelhaupt, E. J. Baerends, C. Fonseca Guerra, S. J. A. van Gisbergen, J. G. Snijders, T. Ziegler, *J. Comput. Chem.* **2001**, *22*, 931.
[65] L. Zhao, S. Pan, N. Holzmann, P. Schwerdtfeger, G. Frenking, *Chem. Rev.* **2019**, *119*, 8781.
[66] P. Pyykkö, *J. Phys. Chem. A* **2015**, *119*, 2326.
[67] P. Pyykkö, M. Atsumi, *Chem. – Eur. J.* **2009**, *15*, 186.
[68] C. Chen, C. G. Daniliuc, G. Kehr, G. Erker, *Angew. Chem. Int. Ed.* **2021**, *60*, 19905.
[69] M. Trose, D. B. Cordes, A. M. Z. Slawin, A. Stasch, *Eur. J. Inorg. Chem.* **2020**, *2020*, 3811.
[70] A. Hock, L. Werner, M. Riethmann, U. Radius, *Eur. J. Inorg. Chem.* **2020**, *2020*, 4015.
[71] M. M. Wu, A. M. Gill, L. Yunpeng, L. Yongxin, R. Ganguly, L. Falivene, F. García, *Dalton Trans.* **2017**, *46*, 854.
[72] M. Sugie, H. Takeo, C. Matsumura, *J. Mol. Spectrosc.* **1987**, *123*, 286.
[73] Y. Kawashima, K. Kawaguchi, E. Hirota, *J. Chem. Phys.* **1987**, *87*, 6331.
[74] E. Rivard, W. A. Merrill, J. C. Fettinger, P. P. Power, *Chem. Commun.* **2006**, 3800. https://doi.org/10.1039/B609748K
[75] C. Marquardt, O. Hegen, M. Hautmann, G. Balázs, M. Bodensteiner, A. V. Virovets, A. Y. Timoshkin, M. Scheer, *Angew. Chem. Int. Ed.* **2015**, *54*, 13122.
[76] W. Lu, H. Hu, Y. Li, R. Ganguly, R. Kinjo, *J. Am. Chem. Soc.* **2016**, *138*, 6650.
[77] T. Jian, L. F. Cheung, T.-T. Chen, L.-S. Wang, *Angew. Chem. Int. Ed.* **2017**, *56*, 9551.
[78] J. Li, X. Li, W. Huang, H. Hu, J. Zhang, C. Cui, *Chem. – Eur. J.* **2012**, *18*, 15263.
[79] R. L. Wells, A. T. McPhail, J. A. Laske, P. S. White, *Polyhedron* **1994**, *13*, 2737.
[80] R. J. Wehmschulte, P. P. Power, *J. Am. Chem. Soc.* **1996**, *118*, 791.
[81] A. Hauser, L. Münzfeld, P. W. Roesky, *Chem. Commun.* **2021**, *57*, 5503.
[82] V. K. Greenacre, W. Levason, G. Reid, *Organometallics* **2018**, *37*, 2123.
[83] C. J. Carmalt, *Coord. Chem. Rev.* **2001**, *223*, 217.
[84] P. V. Muhasina, P. Parameswaran, *ChemistrySelect* **2021**, *6*, 9911.
[85] J. E. Walley, L. S. Warring, E. Kertész, G. Wang, D. A. Dickie, Z. Benkő, R. J. Gilliard Jr., *Inorg. Chem.* **2021**, *60*, 4733.
[86] T. J. Lee, J. E. Rice, G. E. Scuseria, H. F. Schaefer, *Theor. Chim. Acta* **1989**, *75*, 81.
[87] T. J. Lee, P. R. Taylor, *Int. J. Quantum Chem.* **1989**, *36*, 199.

SUPPORTING INFORMATION

Additional supporting information can be found online in the Supporting Information section at the end of this article.

How to cite this article: A. Kaur, D. J. D. Wilson, *J. Comput. Chem.* **2022**, *43*(29), 1964. https://doi.org/10.1002/jcc.26995